

# Structure, current efficiency, and corrosion properties of brush electrodeposited (BED) Cr from Cr(III)dimethyl formamide (DMF)-bath

G. Saravanan · S. Mohan

Received: 21 November 2008 / Accepted: 8 June 2009 / Published online: 19 June 2009  
© Springer Science+Business Media B.V. 2009

**Abstract** Chromium electrodeposited from Cr(III)dimethyl formamide-bath was studied using brush electrodeposition (BED) technique. The effects of current density and plating time on thickness and current efficiency were studied. An advantage of BED Cr was to produce selective area deposition on a suitable substrate. Chromium deposits were characterized using XRD, SEM, and AFM. From the electrochemical studies, BED Cr have higher charge transfer resistance  $R_{ct}$  and very low  $I_{corr}$  than that of mild steel substrate.

**Keywords** Brush electrodeposition · Cr coatings · Dimethylformamide · Metal coatings · Electrochemical impedance spectroscopy (EIS) · Electrodeposited film · Passivity

## 1 Introduction

Chromium is used in industry because of its excellent wear, corrosion resistance, and attractive appearance [1, 2]. The main advantages of Cr(III) electroplating bath in comparison with a Cr(VI) bath is that  $Cr^{3+}$  ions are non-toxic and environmentally benign [3]. However, it is almost impossible to deposit the Cr coating from a simple aqueous Cr(III) solution due to a very stable  $[Cr(H_2O)_6]^{3+}$  complex [4]. According to the published data [5], the slow deposition rate in Cr(III) chloride electrolyte is related to the appearance of very stable  $\mu$ -hydroxo-bridged oligomeric species of Cr(III). To destabilize the strong hexa-aqua

chromium(III) complex, some of the complexing agents [dimethyl formamide (DMF), urea, formic acid, acetate, glycine sodium citrate, DL-aspartic acid, etc.] may be used [6–10]. Chromium plating from Cr(VI) solution is now under pressure due to its toxicity and carcinogenicity; therefore, significant efforts have been applied to the development of alternative process for chromium plating from Cr(VI)-bath [11–13]. LDC-HTC [14] chrome is a first trivalent chrome that produces longer lasting deposits, increased solution life, improves parts wearability and is environmentally friendly. LDC-HTC chrome does not contain or produce hexavalent chrome. This reduces costs and difficulties associated with the disposal of hexavalent waste. This study is important in terms of a Cr(VI)-free process, using Cr(III)DMF-bath as an alternate bath. Therefore, the aim of this study was to develop brush electrodeposition (BED) Cr using a Cr(III)DMF-bath. The corrosion behavior was analyzed in 3.5%NaCl solution using potentiodynamic polarization and electrochemical impedance spectroscopy.

## 2 Experimental

### 2.1 Electrolyte and BED

BED Cr was prepared from a DMF bath consisting of  $212 \text{ g L}^{-1} CrCl_3 \cdot 6H_2O$ ,  $26 \text{ g L}^{-1} NH_4Cl$ ,  $36 \text{ g L}^{-1} NaCl$ ,  $40 \text{ g L}^{-1} B(OH)_3$ , and 200 mL of DMF. AR grade chemicals and distilled water were used to prepare the solution. The effect of current density and time on thickness and current efficiency were studied. The pH of these solutions was adjusted to  $2 \pm 0.2$  by adding HCl/KOH. BED equipment includes power packs, solutions and plating tools, anode covers, and auxiliary equipment.

G. Saravanan · S. Mohan (✉)  
Central Electrochemical Research Institute,  
Karaikudi 630006, India  
e-mail: sanjnamohan@yahoo.com

Microprocessor-controlled selectron power pack Model 150A-40V was used to transform AC current to DC current. The schematic of the brush plating system is given in Fig. 1. The power packs have two leads, one is connected to the plating tool and the other is connected to the work piece to be electrodeposited. The anode is covered with an absorbent material, which holds the solution. The operator dips the plating tool in the solution and then brushes it against the surface of the work piece that is to be finished. When the anode touches the work surface a circuit is formed and deposit is produced. The brush deposits with the thickness of about  $15\ \mu\text{m}$  were obtained at current density of  $24\ \text{A dm}^{-2}$  in 20 min. Mild steel (MS) and BED Cr were represented by (MS) and Cr-(brush)/MS.

## 2.2 Corrosion measurements

### 2.2.1 Cell apparatus

Corrosion measurements were performed in a three-electrode cell with the volume of 150 mL. The samples (MS) and Cr-(brush)/MS were used as the working electrode. A platinum foil and a saturated calomel electrode (SCE) were used as the auxiliary electrode and reference electrode, respectively. The electrodes were connected to a potentiostat (PARSTAT 2273). The corrosion parameters were obtained with in-built software package (powerCORR). All potentials were measured with reference to SCE.

### 2.2.2 Electrochemical procedures

Corrosion behavior was examined in neutral 3.5%NaCl solution at  $30 \pm 1\ ^\circ\text{C}$ . Potentiodynamic polarization curves were measured for all the samples between  $-0.8$  and  $-0.2\ \text{V}$  at a scan rate of  $5\ \text{mV s}^{-1}$ . Impedance spectra were conducted at open-circuit potential over a frequency

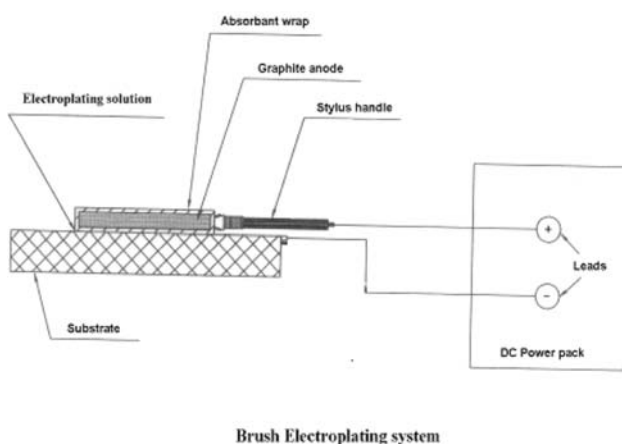


**Fig. 1** Schematic of brush electroplating process

ranging from  $10^5$  to  $10^{-2}\ \text{Hz}$ . The amplitude of potential modulation was 5 mV. All the recorded impedance spectra were shown as Bode and Nyquist diagrams.

## 3 Results and discussion

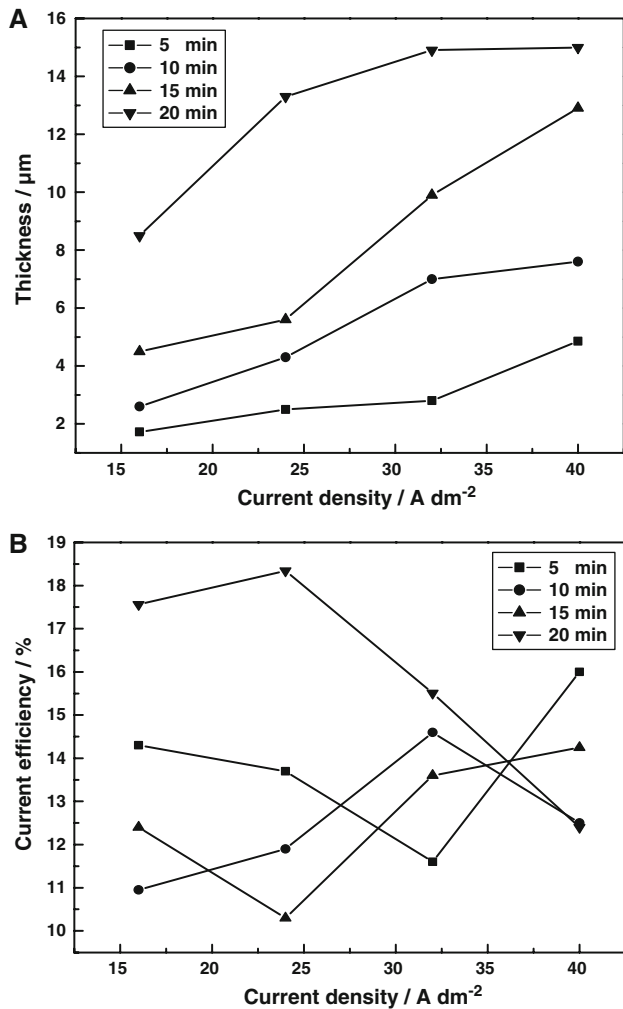
### 3.1 Effect of current density and time on thickness and current efficiency of Cr deposits

Figure 2a shows the effect of current density on the thickness of Cr deposits obtained for various time intervals. From this figure, it is observed that the thickness of the chromium deposit increases with increasing current density and time. When current density and time increased, the amount of current flowing is also increased and so the overall amount of deposition is increased. The maximum thickness ( $15\ \mu\text{m}$ ) was obtained at a current density of  $32\ \text{A dm}^{-2}$  in 20 min. From this figure, the optimum current density and plating time can be fixed for appropriate thickness required. Figure 2b shows the effect of current density on the current efficiency of Cr deposits obtained for various time intervals. From this figure, it is observed that the current efficiencies (18) reach maximum at  $24\ \text{A dm}^{-2}$  in 20 min. In BED system, hydrogen evolution is somewhat low; most of the current supplied is utilized for deposition of chromium, so current efficiency increases with increasing time. When current density increased beyond  $24\ \text{A dm}^{-2}$  burnt deposit occurred. Therefore, from Fig. 2b, we concluded that  $24\ \text{A dm}^{-2}$  is the optimum current density for obtaining maximum current efficiency.

### 3.2 Microstructural characteristics

Morphology of BED Cr on MS substrate was examined under a scanning electron microscopy (SEM). Figure 3a is an SEM photograph of the brush plated chromium after 20 min of deposition and at a current density of  $24\ \text{A dm}^{-2}$ . The deposits exhibited fine-grained, smooth surface nodular structures with nodular size ranging from 1 to  $2\ \mu\text{m}$ . Deposits were brighter, smoother with microcracks. The smaller grains are due to low hydrogen evolution during deposition process [15].

The surface topography of brush-plated Cr was studied using atomic force microscopy (AFM). AFM pictures scanned over an area of  $1 \times 1\ \mu\text{m}^2$  shown in Fig. 3b. The advantage of AFM is its capacity to probe minute details to the individual grains and inter-grain regions. Figure 3b shows the deposit consists of many small spherical particles may be conditioned by progressive nucleation and very low hydrogen evolution during deposition process. From the horizontal cross-section analysis, the minimum



**Fig. 2 a, b** Effect of current density on thickness and current efficiency of deposit in different time

and maximum globule size was estimated to be in the range of 5 to 15 nm.

The XRD patterns of electrodeposited chromium are shown in Fig. 3c. All the electrodeposits consist of grains with strong Cr(110) plane and weak Cr(211) plane for Cr coatings. Crystallite size is assessed by the Debye–Scherrer equation. The values of texture coefficient  $T_C$  ( $\phi$ ) and grain size are tabulated in Table 1. In addition, a relatively strong (110) texture is associated with smaller grain size. The nucleation and growth interface by hydrogen changes the

**Table 1** Texture coefficient and crystallite size of brush-plated chromium

<i>hkl</i>	$2\theta$	$D$ (Å)	$I/I_0$	$T_C$ ( $\phi$ )	Grain size (nm)
Cr(110)	44.6230	2.0306	1	71.65	47.4
Cr(211)	82.3499	1.1700	0.3956	28.34	47.5

surface energy and growth mechanism, and then facilitates the formation of smaller grain size [15].

### 3.3 Corrosion examinations

#### 3.3.1 Potentiodynamic polarization tests

Figure 4a shows potentiodynamic polarization curves for BED Cr in 3.5%NaCl solution. All the curves display the active passive behavior between  $-0.8$  and  $-0.2$  V. It indicates that the mechanism of activity and passivation behavior for Cr-(brush)/MS. The current density increases with increasing potential at the activation region. And then the electrode passivates and displays high stability, as characterized by low and steady value of passive current density. The corrosion current density ( $I_{corr}$ ) and corrosion potential ( $E_{corr}$ ) are calculated from the intercept of the Tafel slops. The corrosion rate (CR) in mils per year was estimated from the polarization curves, and is given in Table 2. Among both the samples Cr-(brush)/MS exhibit the lowest values of  $I_{corr}$  and CR than that of samples MS. Therefore, sample Cr-(brush)/MS exhibits the best corrosion resistance, which is attributed to the compact microstructure.

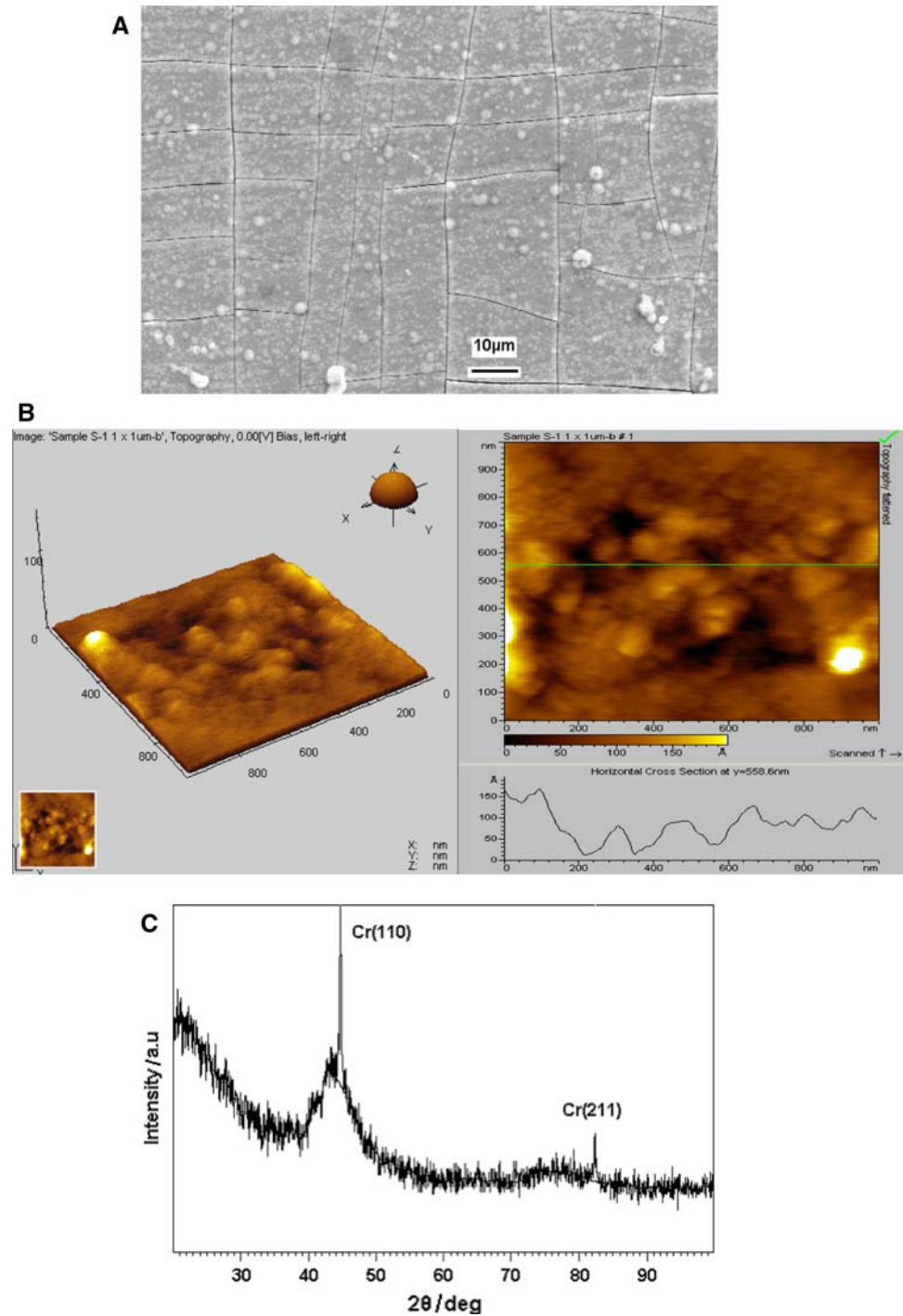
#### 3.3.2 Electrochemical impedance spectra tests

The measured impedance spectra for the electrodeposits in 3.5%NaCl solution are shown as Bode and Nyquist diagrams in Fig. 4b, c. The impedance plots exhibit depressed semicircles. The equivalent circuit as shown in Fig. 4d is used to fit the corrosion resistance parameters.  $R_{ct}$  and  $C_{dl}$  represent the charge-transfer resistance and double layer capacitance, respectively. The fitted impedance spectra are in good agreement with the impedance spectra recorded during the measurements as shown in Fig. 4. The calculated values of circuit elements are listed in Table 3. It can be found that all fitted corrosion parameters of the electrodeposits vary with the changes of the microstructure. The corrosion resistance ( $R_{ct}$ ) of Cr-(brush)/MS is greater than that of MS samples. The increased  $R_{ct}$  values and decreased  $C_{dl}$  values for Cr-(brush)/MS deposits clearly confirm the better corrosion resistance than the MS substrates. Also it is observed a more pronounced semicircular region in the case of Cr-(brush)/MS has maximum corrosion resistance than MS as observed from the high-frequency region of the impedance spectra.

#### 3.3.3 Porosity of Cr-(brush)/MS systems

It is possible to determine the porosity of a coating using an electrochemical measurement technique that determines the ratio of the current density through the pores and the

**Fig. 3** SEM (a) AFM (b) of BED Cr deposits at  $24 \text{ A dm}^{-2}$ . c XRD patterns of brush-plated chromium at  $24 \text{ A dm}^{-2}$



coating [16]. Using the facts that when determining the porosity, in most cases the cathodic current is negligible, and the current density is inversely proportional to the polarization resistance. Elsener et al. [17] estimated the porosity of TiN-coated MS from the shift of the corrosion potential caused by the presence of the coating ( $\Delta E_{\text{corr}}$ ) and

from the polarization resistance of the brush-plated coating ( $R_p$ ) and the substrate material ( $R_{p,s}$ ) as given below [18].

$$P = \left( \frac{R_{p,s}}{R_p} \right) \times 10^{-|\Delta E_{\text{corr}}|/b_a},$$

where  $b_a$  is the Tafel slope of the active dissolution of MS.

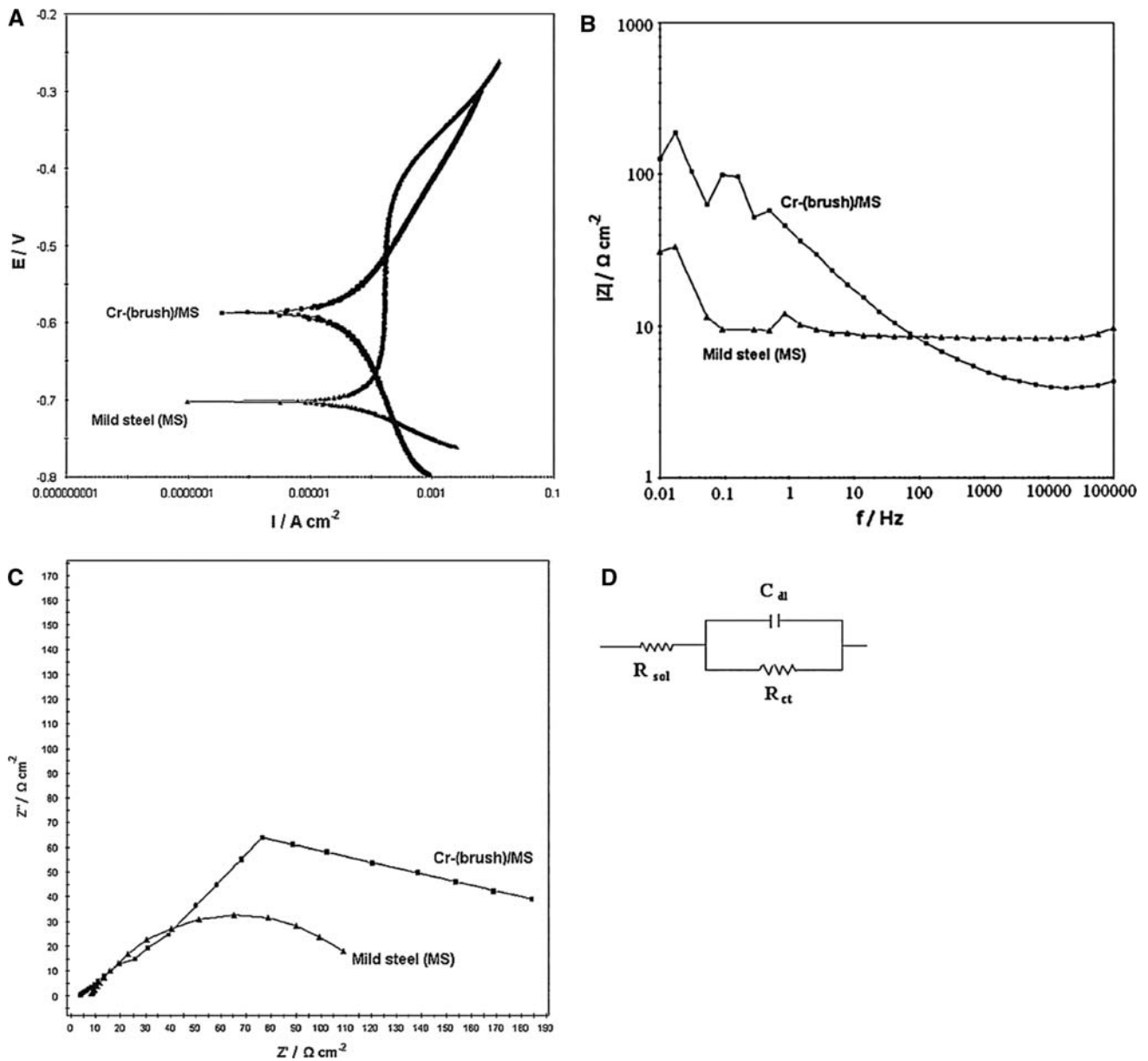


**Fig. 4** **a** Polarization curve of brush-plated chromium in 3.5%NaCl solution. Impedance spectra for BED Cr in 3.5%NaCl solution in **b** Bode diagram and **c** Nyquist diagram and **d** equivalent circuit diagram of impedance spectra for brush-plated chromium in 3.5%NaCl solution

**Table 2** Corrosion parameters obtained from polarization studies in 3.5% w/v NaCl solution

Sample	$E_{\text{corr}}$ versus SCE (mV)	$b_a$ (V/decade)	$b_c$ (V/decade)	$I_{\text{corr}}$ ( $\text{A cm}^{-2}$ )	CR ( $\text{mm y}^{-1}$ )
MS panel	-0.702	0.388	-0.056	$2.5 \times 10^{-4}$	1.9304
Cr-(brush)/MS	-0.587	0.214	-0.214	$5.6 \times 10^{-5}$	0.4318

Using this equation, and the values of ( $R_{p,s}$ ) ( $102.5 \Omega \text{ cm}^2$ ) and  $b_a$  (0.483 V/decade) determined from separate measurement on an uncoated MS substrate in 3.5%NaCl solution, we estimate the porosity of the Cr-(brush)/MS systems. For

this purpose, the  $E_{\text{corr}}$  of the MS was determined to be -702 mV vs. SCE. The coating porosity determined in this way was approximately 0.162% for the Cr (brush)/MS in 3.5%NaCl solution. From this value, BED Cr coating system

**Table 3** Corrosion parameters obtained from impedance measurements by Bode and Nyquist plots

Sample	OCP (V)	$R_{ct}$ ( $\Omega \text{ cm}^2$ )	$C_{dl}$ ( $\text{F cm}^{-2}$ )	Porosity (%)
MS panel	-0.547	102	163.4	–
Cr-(brush)/MS	-0.543	194	25.8	0.162

is having lower porosity than that reported in the literature [18]. Therefore, Cr-(brush)/MS have better corrosion resistance system than that of MS substrate.

#### 4 Conclusions

- (1) Cr(III)DMF-based electrolyte was developed from which effect of current density and plating time were studied. Thickness and current efficiency is increased because of lower hydrogen evolution. Thickness and current efficiency of Cr deposit is reached maximum of  $15 \mu\text{m}$  at  $32 \text{ A dm}^{-2}$  and  $18 \mu\text{m}$  at  $24 \text{ A dm}^{-2}$ , respectively.
- (2) Corrosion measurements show appreciable increase in corrosion resistance for BED Cr from Cr(III)DMF-bath than that of the MS.
- (3) SEM, AFM, and XRD images of BED Cr show fine-grained nodular and microcrystalline deposit.

**Acknowledgment** One of the authors thanks the Department of Science and Technology New Delhi for a research grant under SERC (Engineering Sciences) scheme no. SR/S3/ME/047/2005.

#### References

1. Zhixiang Z, Junyan Z (2008) *Surf Coat Technol* 202(12):2725
2. Nam K-S, Lee K-H, Kwon S-C, Lee DY, Song Y-S (2004) *Mater Lett* 58:3540
3. Kwon S-C, Lee H-J, Kim J-K, Eungsun B, George C, Ken S (2007) *Surf Coat Technol* 201(15):6601
4. Li B, Lin A, Gan F (2006) *Surf Coat Technol* 201(6):2578
5. Ibrahim SK, Gawne DT, Watson A (1998) *Trans Inst Met Finish* 76(4):156
6. Surviliene S, Jasulaitiene V, Nivinskiene O, Cesuniene A (2007) *Appl Surf Sci* 253(16):6738
7. Hwang J-Y (1991) *Plat Surf Finish* 78(5):118
8. El-Sharif M, McDougall J, Chisholm CU (1999) *Trans Inst Met Finish* 77(4):139
9. Song YB, Chin D-T (2002) *Electrochim Acta* 48(4):349
10. Mandich NV (1997) *Plat Surf Finish* 84(5):108
11. El-Sharif M, Chisholm CU (1997) *Trans Inst Met Finish* 75:208
12. Ward JJB, Christie IRA (1971) *Trans Inst Met Finish* 49:148
13. Robert B (1983) AES 10th plating in the electronics industry symposium, San Francisco Hilton, San Francisco, CA, 1–2 February 1983, pp 199–205
14. [www.ldcbrushplat.com](http://www.ldcbrushplat.com)
15. Haug K, Jenkins T (2000) *J Phys Chem B* 104:10017
16. Tato W, Landolt D (1998) *J Electrochem Soc* 145:4173
17. Elsener B, Rota A, Bohni H (1989) *Mater Sci Forum* 29:44
18. Merl DK, Panjan P, Cekada M, Macek M (2004) *Electrochim Acta* 49:1527